# Downregulation of FUSE-binding protein and c-myc by tRNA synthetase cofactor p38 is required for lung cell differentiation

Min Jung Kim[1], Bum-Joon Park[1], Young-Sun Kang[1], Hyoung June Kim[1], Jae-Hyun Park[1], Jung Woo Kang[1], Sang Won Lee[1], Jung Min Han[2], Han-Woong Lee[3] & Sunghoon Kim[1]

p38 is associated with a macromolecular tRNA synthetase complex[1]. It has an essential role as a scaffold for the complex, and genetic disruption of p38 in mice causes neonatal lethality[2]. Here we investigated the molecular mechanisms underlying lethality of p38-mutant mice. p38-deficient mice showed defects in lung differentiation and respiratory distress syndrome. p38 was found to interact with FUSE-binding protein (FBP), a transcriptional activator of c-myc[3]. Binding of p38 stimulated ubiquitination and degradation of FBP, leading to downregulation of c-myc, which is required for differentiation of functional alveolar type II cells. Transforming growth factor-β (TGF-β) induced p38 expression and promoted its translocation to nuclei for the regulation of FBP and c-myc. Thus, this work identified a new activity of p38 as a mediator of TGF-β signaling and its functional importance in the control of c-myc during lung differentiation.

Alveolar type II cells are important for pulmonary respiration because they secrete surfactants that reduce the surface tension of water on the alveolar surface. Incomplete differentiation of these cells may cause respiratory distress syndrome, which occurs frequently in pre-term infants and is a principal cause of their death. Here we report that p38 has an important role in the differentiation of alveolar type II cells by downregulating FBP and c-myc. p38 was first identified as a factor associated with a macromolecular protein complex consisting of several different aminoacyl-tRNA synthetases and was also independently reported as JTV-1 protein[4]. We previously showed that p38 is a scaffold required for the assembly and stability of the multi-tRNA
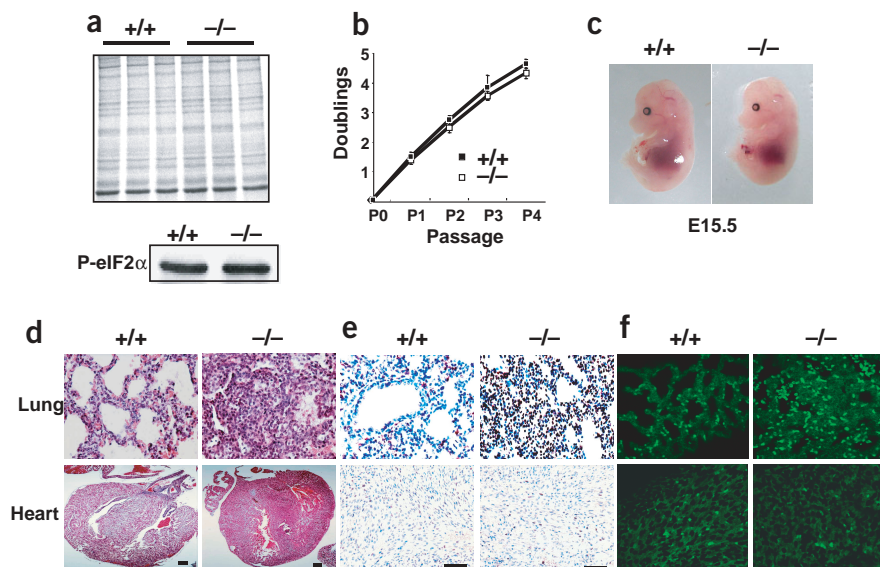
Figure 1 Protein synthesis, cell growth and histological characteristics of p38-deficient mice. (**a**) We compared overall protein synthesis in wild-type and p38-deficient MEFs by autoradiography of the [^{35}S]-methionine incorporated into nascent proteins (upper) and also by the phosphorylation of eIF2α (P-Eif2α; lower). (**b**) We compared growth rates of wild-type and p38-deficient MEFs ($n = 3$ for each genotype). (**c**) Gross morphology of E15.5 wild-type and p38-deficient embryos. (**d**) Hematoxylin and eosin staining of lung and heart tissues isolated from neonatal mice. (**e**) Immunohistochemical staining of lung and heart sections with antibody to PCNA (dark brown). The sections were counterstained with 50% dilution of Harry's hematoxylin (blue). (**f**) Immuno-fluorescence staining of lung and heart sections with antibody to Ki67. The Ki67-positive cells were detected by confocal laser scanning microscopy (green). Scale bars = 12.5 μm, except scale bar in hematoxylin and eosin staining of heart = 25 μm.

[1]National Creative Research Initiatives Center for ARS Network, College of Pharmacy, Seoul National University, Seoul 151-742, Korea. [2]Imagene, Biotechnology Incubation Center, Seoul National University, Seoul 151-742, Korea. [3]Sungkyunkwan University School of Medicine, Samsung Biomedical Research Institute, Suwon 440-746, Korea. Correspondence should be addressed to S.K. (sungkim@snu.ac.kr).

Figure 2 Defect in the differentiation of alveolar type II cells and surfactant production in lungs of p38-deficient mice. (**a**) Lung morphology of wild-type and p38-deficient mice at E18.5 and P1. Scale bar = 50 μm. (**b**) Level of HIF-1α in brains of P1 mice. Tubulin was used as a loading control. (**c**) We determined the production of the lung surfactant proteins (SP-A, SP-B and SP-C) in the proteins extracted from the neonatal lungs by western blotting. (**d,e**) Immunofluorescence staining of lung alveolar sections with the antibodies to SP-B (**d**) and SP-C (**e**; green). The nuclei were stained with propidium iodide (red). Scale bar = 10 μm.
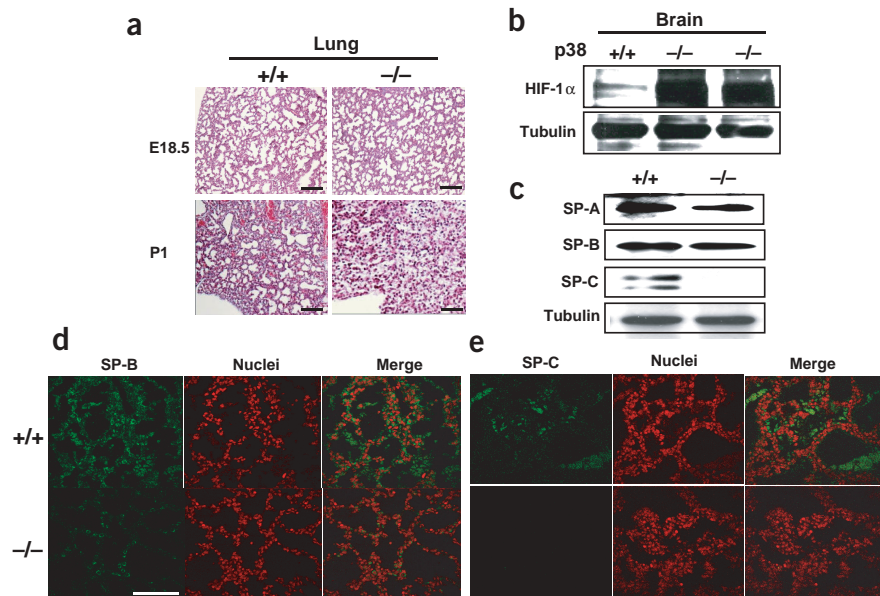

synthetase complex[2]. Notably, mice that are homozygous, but not heterozygous, with respect to mutations in *Ahsa1* (encoding p38) showed neonatal lethality, although they were born alive with the normal segregation ratio. In this work, we carried out experiments to identify the activity of p38 that is related to the lethality of the mutant mice.

We first checked whether deficiency of p38 affected global protein synthesis and cell growth in mouse embryonic fibroblasts (MEFs). We monitored protein synthesis by autoradiography of the nascent polypeptides and phosphorylation of eIF2α, which controls translational initiation[5], and monitored cell growth by the serial passage of MEFs. The p38-deficient cells showed little difference in protein synthesis (**Fig. 1a**) and growth rate compared with the normal cells (**Fig. 1b**). In addition, the mutant embryos had no apparent distinction in size or gross morphology (**Fig. 1c**). The histological analyses, however, showed severe hyperplasia in various organs, including lung, intestine and liver, of the p38-deficient mice (**Fig. 1d** and data not shown). To verify this observation, we immunostained the lung tissues with antibodies against the cell proliferation markers PCNA (proliferating cell nuclear antigen) and Ki67 (ref. 6). The lungs of mutant mice were heavily stained with these antibodies, whereas the hearts of mutant mice showed no apparent difference relative to the wild-type tissues (**Fig. 1e,f**).

We further examined the lungs of mutant mice because lung failure could be the direct cause of their neonatal lethality. Lungs of wild-type mice had normal alveoli structures at both the pre- and postnatal stages, but the lungs of the postnatal mutant mice were collapsed (**Fig. 2a**) and the level of hypoxia-inducible factor 1α (HIF-1α) was highly elevated in the mutant brains[7] (**Fig. 2b**), implicating lung dysfunction. Lung collapse is often caused by a lack of surfactants on the surface of alveoli[8]. Among the lung surfactants, SP-B and SP-C control surface tension on the alveolar surface[9], and SP-A and SP-D are involved in immune response[10]. We compared the levels of different surfactants in the lungs of normal and p38-deficient mice by western blotting. SP-C, which is specifically generated from alveolar type II cells[11], was not detected in the lungs of mutant mice, whereas SP-A and SP-B, which are produced from different lung cells[12], were present in slightly smaller amounts relative to wild-type (**Fig. 2c**). Immunofluorescence staining showed markedly smaller amounts of SP-B and SP-C in the alveolar surface of

Figure 3 Interaction of p38 with FBP. (**a**) We determined the interaction of p38 with the indicated proteins by yeast two-hybrid assay. KRS, WRS, YRS and QRS stand for lysyl-, tryptophanyl-, tyrosyl- and glutaminyl-tRNA synthetase, respectively. Positive interactions are indicated by the formation of blue colonies on YPD medium containing 5-bromo-4-chloro-3-indolyl-b-D-galactoside. (**b**) Top: The proteins that were copurified with GST (G) or GST–p38 (Gp) were separated by SDS–PAGE. A protein of about 68 kDa was specifically detected from the proteins copurified with GST–p38. Middle: We identified this protein by peptide fingerprinting using MALDI–TOF analysis. The peptides that match with parts of mouse FBP (GI15928578) are underlined. Bottom: The copurification of FBP with GST–p38 was confirmed by western-blot analysis with antibody to FBP. WCL, whole-cell lysate. (**c**) Top: Coimmunoprecipitation of myc–p38 and HA–FBP in 293 cells. IP, immunoprecipitation; WCL, whole-cell lysate. Bottom: Coimmunoprecipitation of endogenous p38 and FBP in 293 cells.
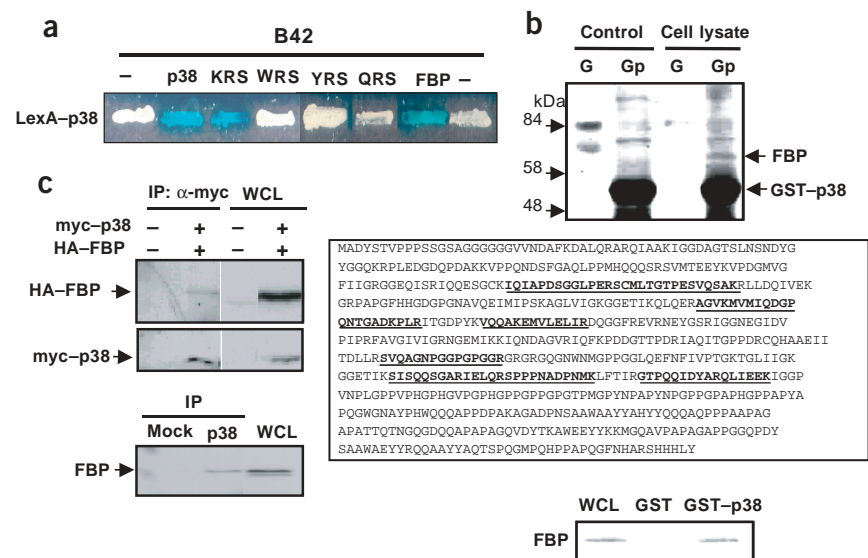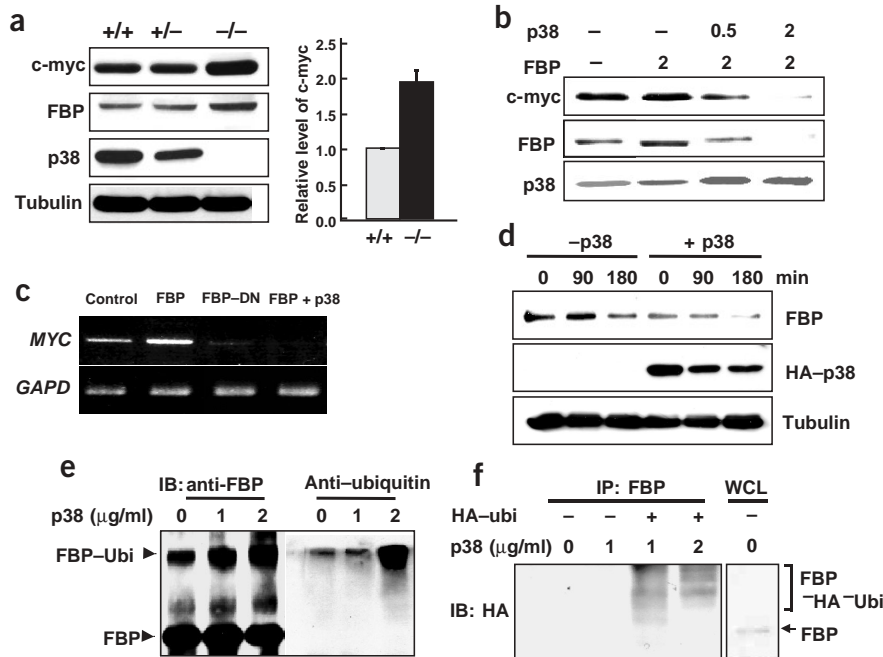
Figure 4 p38-dependent ubiquitination and degradation of FBP. (**a**) Levels of c-myc, FBP and p38 in the lungs of neonatal littermates. The bar graph indicates the relative levels of c-myc in the lungs of wild-type and p38-deficient mice ($n = 7$ each). (**b**) The increase of the p38 level by transient transfection (0, 0.5 and 2 µg of the p38 plasmid) decreased the levels of FBP and c-myc in 293 cells. (**c**) We determined the effect of FBP and p38 on the expression of *Myc* by RT–PCR. *Gapd* was used as a loading control. (**d**) The p38-stimulated degradation of FBP in 293 cells treated with cycloheximide. The FBP level was monitored by western blotting at the indicated times after the cycloheximide treatment. (**e**) The p38-dependent ubiquitination of FBP in 293 cells treated with ALLN (26S proteasome inhibitor). We introduced the indicated amounts of the p38 plasmid into the cells, immunoprecipitated (IP) the proteins extracted from the cells with antibody to FBP and immunoblotted (IB) them with antibodies to FBP and ubiquitin (Ubi). (**f**) We also determined the ubiquitination of FBP by the coexpression of HA–ubiquitin with different amounts of the p38 plasmid in 293 cells. Ubiquitinated FBP was detected by western blotting with the antibody to hemagglutinin (HA). WCL, whole-cell lysate.

the lungs of mutant mice (**Fig. 2d,e**), however, suggesting a defect in the differentiation of the functional type II cells. Thus, we concluded that lung failure is the direct cause of the lethality of the mutant mice.

To determine the working mechanism of p38, we screened for p38-binding proteins using yeast two-hybrid assays. The screen identified p38, lysyl-tRNA synthetase (KRS) and FBP (data not shown), and we confirmed their interactions with p38 using the full-length polypeptides (**Fig. 3a**). FBP was also copurified with a glutathione S-transferase (GST)–p38 fusion protein from the proteins extracted from mouse brain expressing FBP at a high level[13] (**Fig. 3b**). The cellular interaction of the two proteins was also shown by coimmunoprecipitation between the exogenously introduced myc-tagged p38 (myc–p38) and hemagglutinin-tagged FBP (HA–FBP) as well as between the endogenous proteins (**Fig. 3c**). *In vitro* binding analyses with deletion fragments of FBP and its isoforms showed that p38 binds to the C-terminal region of FBP, which is responsible for the *trans*-activation activity[14], but not to its N-terminal region of 443 amino acids or to its isoforms, FBP2 and FBP3 (ref. 15; **Supplementary Fig. 1** online).

To understand the function of the interaction between p38 and FBP, we compared the levels of FBP and c-myc in the lungs of the neonatal littermates. Levels of FBP and c-myc were higher in the lungs of the homozygous mutant mice than in those of their wild-type and heterozygous littermates (**Fig. 4a**). The transcript level of FBP was unchanged by the deficiency of p38, however, indicating that p38 does not affect the transcription of FBP (data not shown). Transient transfection with p38 caused a reduction in the levels of FBP and c-myc (**Fig. 4b**). The effect of p38 on expression of c-myc was also monitored by RT–PCR. Expression of c-myc is enhanced by FBP and blocked by the dominant negative form of FBP[14]. Coexpression of p38 abolished the FBP-dependent induction of c-myc (**Fig. 4c**). p38 promoted the turnover of FBP in 293 cells treated with cycloheximide (**Fig. 4d**).

We then examined whether ubiquitination is involved in the p38-dependent degradation of FBP using N-acetyl-Leu-Leu-norleucinal (ALLN), which blocks the 26S proteasome[16]. In 293 cells treated with

ALLN, the level of FBP was not reduced by p38 (**Fig. 4e**). In addition, the higher molecular weight bands of FBP accumulated with greater amounts of p38, and these bands reacted with the antibody to ubiquitin (**Fig. 4e**), indicating that they represented ubiquitinated FBP. The ubiquitination of FBP was enhanced by coexpression of p38 with hemagglutinin-tagged ubiquitin (**Fig. 4f**). Experiments using the deletion fragments of p38 showed that the ability of p38 to bind FBP is essential for the ubiquitination of FBP and suppression of c-myc (**Supplementary Fig. 2** online).

We then used transient transfection to check whether p38 affects cell proliferation. p38 substantially reduced the proliferation of various epithelial carcinoma cell lines, except for human osteosarcoma Saos2 cells (**Fig. 5a**). The anti-proliferative activity of p38 was abolished by coexpression of c-myc with p38 (**Fig. 5b**), implying that p38 controls cell proliferation mainly through c-myc. In lung epithelial primary cells and carcinoma cells, p38 induced the expression of surfactants SP-B and SP-C and suppressed the expression of c-myc (**Fig. 5c**).

Transforming growth factors are involved in lung organogenesis, and the genetic disruption of TGF-β2 or -β3 causes lung failure and postnatal lethality[17,18]. In addition, although p38 suppressed proliferation of the epithelial carcinoma cells, it did not suppress osteosarcoma cells, which are resistant to TGF-β-induced growth arrest (**Fig. 5a**). This prompted us to investigate the functional link between p38 and TGF-β signaling by determining whether the level of p38 is affected by TGF-β. Treatment with TGF-β2 increased the level of p38 in 293 and DU145 cells but not in HCT116 cells, which lack the type II TGF-β receptor[19] (**Fig. 5d**). The TGF-β-dependent increase of p38 suppressed FBP and c-myc and restored the production of SP-C (**Fig. 5e**). To see if p38 is actually involved in TGF-β signaling, we examined the induction of the target proteins p15 (ref. 20) and fibronectin[21] after treating normal and p38-deficient cells with TGF-β. The genes encoding these proteins did not respond to TGF-β in the mutant cells (**Fig. 5f**), showing the functional importance of p38 in the TGF-β signal pathway.

p38 should be present in the nucleus to bind the transcriptional factor FBP. TGF-β induced nuclear translocation of p38 in A549 cells, as determined by cell fractionation (**Fig. 6a**) and immunofluorescence staining (**Fig. 6b**). We observed similar results in HeLa and DU145 cells as well (data not shown). We then addressed the dynamic relationship between p38 and its target proteins. The yeast two-hybrid analysis showed that different peptide regions of p38 are involved in its interaction with KRS and FBP (**Fig. 6c**). TGF-β did not affect the formation of the multi-tRNA synthetase complex and increased the portion of p38 that is not bound to the multi-tRNA synthetase complex (**Fig. 6d**). These results imply that the binding of p38 to tRNA synthetases in the cytoplasm and to FBP in the nucleus may take place independently. The TGF-β-dependent regulation of c-myc through p38 and its relationship with the multi-tRNA synthetase complex are summarized in **Figure 6e**.

FBP can be negatively controlled by FIR (FBP-interacting repressor), which forms an inhibitory complex with FBP[22]. Here we showed that p38 controls the turnover of FBP by its ubiquitination (**Fig. 4**). p38 may have an additional inhibitory effect because it binds to the C-terminal *trans*-activation domain of FBP[14] (**Supplementary Fig. 1** online). p38 suppresses c-myc but is in turn upregulated by c-myc[23,24]. This regulatory loop may be necessary to check the hyperproliferation resulting from abnormal induction of c-myc. Overexpression of c-myc is frequently associated with cancers in various tissues and organs, including lung, and its expression is suppressed during lung differentiation[25,26].

Thus, the role of p38 in the control of c-myc expression should be important in the functional differentiation of the lung and possibly other organs. In this context, it is worth noting that normal proliferation and differentiation of thymocytes were substantially disturbed in p38-deficient mice (**Supplementary Fig. 3** and **Supplementary Methods** online). The functional importance of p38 in the development of other systems warrants further investigation. In this work, we identified a new activity of p38 as a negative regulator of FBP and c-myc signaling in a pathway triggered by TGF-β.

METHODS

Protein synthesis and cell growth. To compare cellular protein synthesis, we cultivated 1×10^5 fibroblast cells from E14.5 mouse fetuses on six-well culture plates for 12 h and then in methionine-free Dulbecco's modified Eagle medium (DMEM; Sigma) for 30 min. We then transferred the cells to medium containing 2 μCi ml^{-1} of [^{35}S]-methionine (Amersham) and incubated them for 1 h. After washing the cells with phosphate-buffered saline (PBS), we extracted the proteins from the cells, separated them by SDS–PAGE and monitored the incorporation of radioactive methionine by autoradiography. We immunoblotted the extracted proteins with a polyclonal rabbit antibody specific to the phosphorylated form of human eIF2α (Santa Cruz). To determine cell proliferation, we cultivated MEFs in DMEM containing 10% fetal bovine serum and conducted the serial passages according to the 3T3 protocol[27]. In brief, we plated 1×10^6 cells on 10-cm dishes, counted the cells after 3 d and then transferred the same number of cells to fresh medium for the next round of cultivation. We calculated the population doubling number
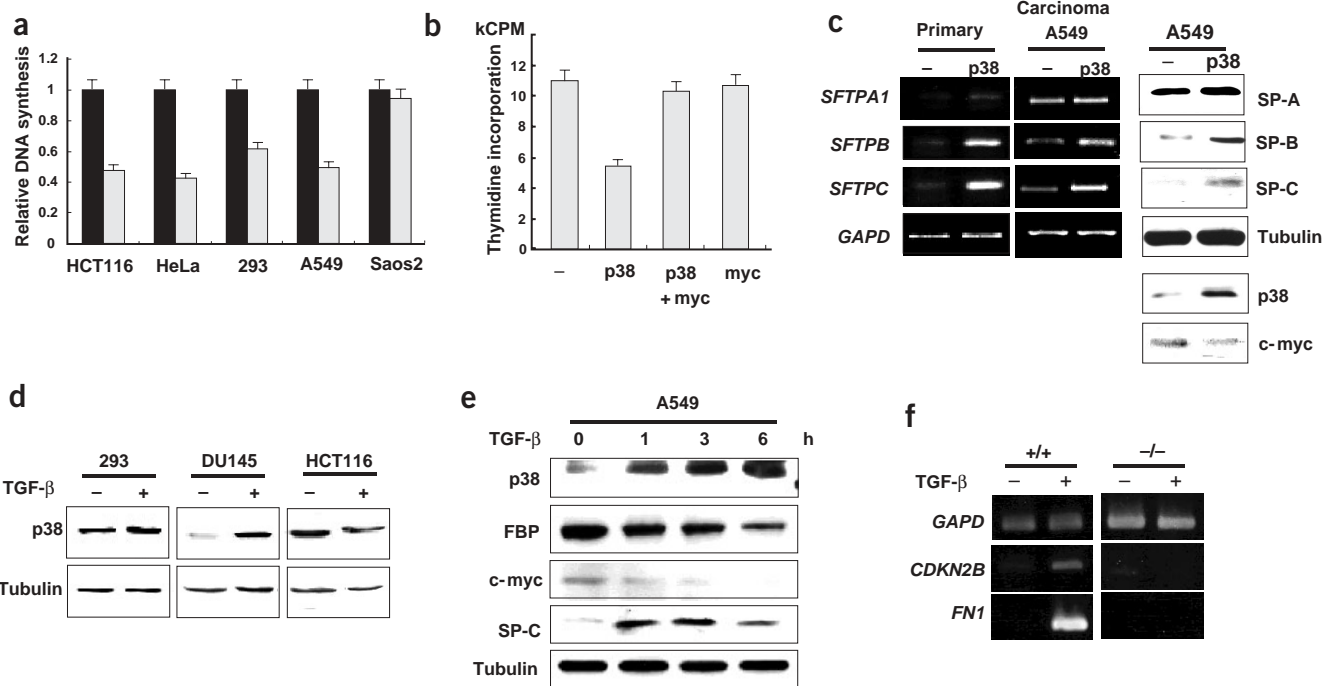
Figure 5 The effect of p38 on cell proliferation and differentiation and its role in the TGF-β signaling pathway. (**a**) The effect of p38 on proliferation of the indicated cell lines. We monitored cell proliferation by the incorporation of radioactive thymidine. (**b**) To see whether the anti-proliferative effect of p38 was relieved by the coexpression of c-myc, we transfected 293 cells with the indicated plasmids and determined cell proliferation. (**c**) The effect of p38 on generation of lung surfactants in the epithelial primary cells and carcinoma A549 cells. We compared production of the surfactants and of p38 and c-myc by RT–PCR (left) and western blotting (right). *GAPD* was used as a loading control for RT–PCR and tubulin as a loading control for western blotting. (**d**) The effect of TGF-β2 on the level of p38 in different cell lines. TGF-β2 did not increase the level of p38 in HCT116 cells, which lack the type II TGF-β receptor. Tubulin was used as a loading control. (**e**) The time course of the TGF-β-dependent increase of p38 in A549 cells. The TGF-β-dependent increase of p38 decreased the levels of FBP and c-myc and restored the production of SP-C. Tubulin was used as a loading control. (**f**) The functional importance of p38 in TGF-β signaling. We compared the expression of the TGF-β target genes, *Cdkn2b* (encoding p15) and *Fn1* (encoding fibronectin), by RT–PCR in normal and p38-deficient MEFs that were treated with TGF-β2. *Gapd* was used as a loading control.

Figure 6 TGF-β induced nuclear translocation of p38. (**a**) Comparison of the p38 level in nuclear and cytoplasmic fractions of A549 cells that were untreated or treated with TGF-β2. PCNA and heat shock protein (HSP) 70 were used as nuclear and cytoplasmic markers, respectively. (**b**) Immunofluorescence staining of p38 in A549 cells with monoclonal antibody to p38. p38 and nuclear DNA were visualized with secondary antibody conjugated to fluorescein isothiocyanate (green) and propidium iodide (red), respectively. (**c**) Identification of the peptide region of p38 that is responsible for interaction with FBP or KRS. Positive interaction was determined by the blue colonies in yeast two-hybrid analysis. (**d**) The effect of TGF-β on formation of the multi-tRNA synthetase complex. We immunoprecipitated (IP) the complex with antibody to p18 from the TGF-β-treated and untreated 293 cells and determined the coprecipitation of p38 and the complex-forming enzyme arginyl-tRNA synthetase (RRS). We then checked the amounts of p18, p38 and arginyl-tRNA synthetase in the immunodepleted (ID) supernatants, which represent the portion of the respective proteins that were not bound to the multi-tRNA synthetase complex. (**e**) Schematic representation of the TGF-β signal pathway including p38, FBP and c-myc required for alveolar type II cell differentiation in lung. p38 is increased and translocated to the nucleus by TGF-β and mediates ubiquitination of FBP, which is a transcriptional activator of c-myc. The ubiquitinated FBP is then subjected to 26S proteasome–mediated degradation, leading to the downregulation of c-myc that is required for lung differentiation. ARS, aminoacyl-tRNA synthetase.
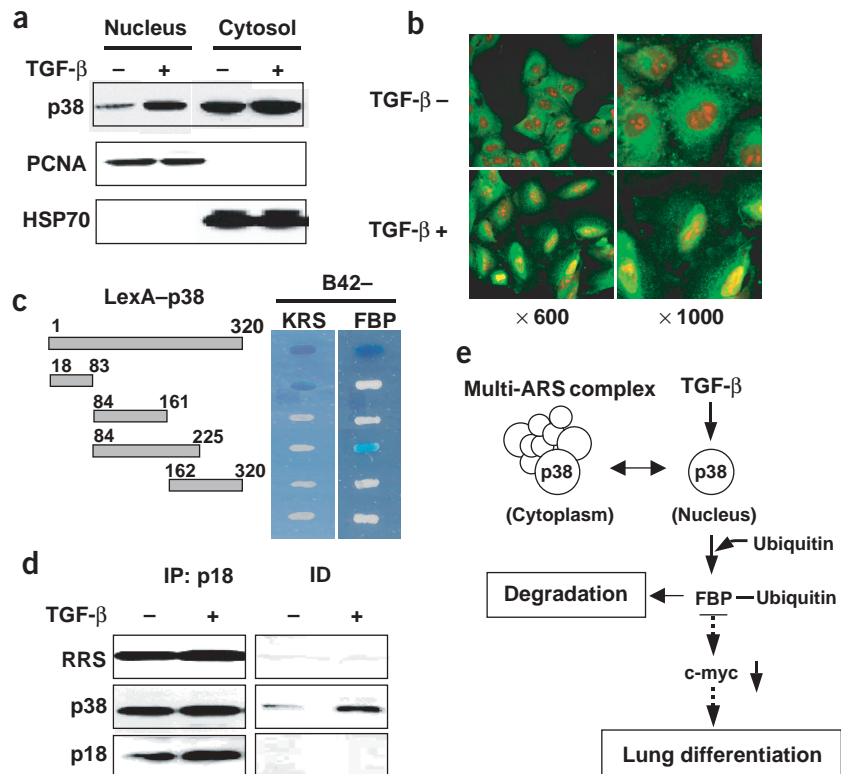
using the formula PDL = log(n_f/n_0)/log2, where n_0 and n_f stand for the initial and final cell numbers, respectively. The animal care and use committee of Seoul National University approved the animal experiments.

Tissue analyses. We isolated various organs from the newborn pups, fixed them with 10% formaldehyde, dehydrated them and embedded them in paraffin. We sliced the embedded tissues by microtome (Leica), mounted them on silane-coated slides, dewaxed them, rehydrated them, stained them with hematoxylin and eosin, and observed them by microscopy (Nikon TE300). We incubated the sliced tissue sections with antibody to PCNA (Zymed) and used a Histomouse-SP Kit based on the biotin-streptavidin-peroxidase system (Zymed) to detect PCNA-positive cells. We also used indirect immunofluorescence staining of the tissue sections with antibody to Ki67 (Santa Cruz). To determine the induction of HIF-1α, we isolated the neonatal mouse brains, extracted proteins and immunoblotted them with antibody to HIF-1α (provided by J.W. Park, Seoul National University, Korea). To detect production of the surfactants, we extracted the proteins from the pre- or postnatal lungs and immunoblotted them with the antibodies specific to surfactants SP-A, SP-B and SP-C (Santa Cruz). We also fixed the isolated lungs with 4% paraformaldehyde at 4 °C overnight, washed them with PBS, incubated them in 30% sucrose for 4 h and finally froze them at −70 °C in optimal cutting temperature (OCT) compound. We attached the frozen sections to silane-coated slides, treated them with 3% hydrogen peroxide in 100% methanol, blocked them with PBS containing 0.1% Tween 20 and 1% skim milk and reacted them with antibodies to SP-B and SP-C for immunofluorescence staining. The nuclei were stained with propidium iodide.

Yeast two-hybrid analysis. We constructed the LexA–human p38 fusion protein and used it as the bait to screen the binding proteins from the human fetal brain cDNA library in which proteins were expressed as B42 fusion proteins. The cDNA encoding the full-length human FBP was provided by D. Levens (US

National Institutes of Health). We obtained the cDNAs encoding human lysyl-, tryptophanyl-, tyrosyl- and glutaminyl-tRNA synthetases (KRS, WRS, YRS and QRS, respectively) from the *Eco*RI and *Xho*I digest of the pLexA vectors containing the corresponding cDNAs[28] and ligated them to the *Eco*RI and *Xho*I sites of the pB42. We tested their interactions with LexA–p38 on medium containing 5-bromo-4-chloro-3-indolyl-b-D-galactoside as described[29]. We prepared the DNAs encoding the different deletion fragments of p38 by PCR using the appropriate primers, expressed them as LexA fusion proteins and tested their interactions with the B42-fused FBP and KRS.

Affinity purification of p38-binding protein. We ligated the cDNA encoding p38 to the *Eco*RI site of pGEX-4T-1 (Amersham) to express the GST–p38 fusion protein in *Escherichia coli* and purified GST and GST–p38 following the manufacturer's instruction. We homogenized adult mouse brains using a polytron homogenizer in 20 mM Tris buffer (pH 7.5) containing 10 mM NaCl, 0.5 mM EDTA and 0.5 mM phenylmethylsulonyl fluoride, centrifuged the homogenate at 100,000*g* for 1 h and adjusted the supernatant to 0.5% Triton X-100. We immobilized GST or GST–p38 to glutathione-sepharose 4B, mixed them with 10 mg of the brain protein extracts at 4 °C for 12 h and then precipitated and washed the beads by brief centrifugation. We eluted the proteins bound to either GST or GST–p38 immobilized to the beads and separated them by SDS–PAGE. We excised one protein band that was specifically copurified with GST–p38, digested it with trypsin (Roche Molecular Biochemicals) at 37 °C for 6 h and determined the masses of the digested peptide fragments using a Voyager DE time-of-flight mass spectrometer (Perceptive Biosystems). The delayed ion extraction resulted in peptide masses with better than 50 ppm mass accuracy on average. We searched the Swiss-Prot database for the protein matching the amino-acid sequences and the mass numbers of the tryptic peptides. We also tested the interaction of p38 with FBP isoforms by *in vitro* pull-down assays as described in **Supplementary Methods** online.

Coimmunoprecipitation. We cleaved the cDNA encoding human p38 from pLexA–p38 with *Eco*RI and *Xho*I and used it to generate the plasmid encoding the myc-tagged p38. We transfected the plasmids encoding myc–p38 and HA–FBP into 293 cells, immunoprecipitated p38 with the antibody to myc, resolved the precipitates by SDS–PAGE and immunoblotted with the antibody to hemagglutinin. To determine the interaction between endogenous p38 and FBP, we coimmunoprecipitated the two proteins from the protein extracts of 293 cells with their specific antibodies. To monitor the assembly of the multi-tRNA synthetase complex, we immunoprecipitated the complex with antibody to p18 and detected the coimmunoprecipitation of p38 and the complex-forming tRNA synthetase, arginyl-tRNA synthetase, by western blotting of the precipitates with their respective antibodies.

RT–PCR. To see the effect of p38 on the expression of c-myc, we carried out quantitative RT–PCR. We transfected 293 cells with 1 μg each of the plasmids encoding FBP, dominant-negative mutant of FBP (FBP-DN) and p38 + FBP. We then isolated the total RNAs from the transfected cells and carried out RT–PCR with the primers specific to the c-myc cDNA. We also applied RT–PCR to analyze expression of the genes encoding p15 and fibronectin in wild-type and p38-deficient MEFs that were untreated or treated with TGF-β2 (2 ng ml^{-1}). To determine the expression of the lung surfactants, we carried out quantitative RT–PCR using pairs of the specific primers. We designed primers for the genes encoding SP-A, SP-B and SP-C to produce DNA fragments of 450, 350 and 290 bp, respectively. The primer sequences and PCR conditions are available on request.

Degradation and ubiquitination of FBP. To determine the effect of p38 on the stability of FBP, we transfected 293 cells with the plasmid encoding p38 (2 μg ml^{-1}), cultivated it for 16 h and blocked *de novo* protein synthesis by treatment with cycloheximide (10 μg ml^{-1}). We then harvested the cells at the indicated times, extracted the proteins and immunoblotted them with antibody to FBP. To determine the p38-dependent ubiquitination of FBP, we treated 293 cells with 15 μg ml^{-1} of ALLN for 3 h to inhibit 26S proteasome and then transfected these cells with the indicated amounts of the p38 plasmid. We then extracted proteins, immunoprecipitated them with antibody to FBP and immunoblotted the precipitates with antibody to FBP and monoclonal antibody to ubiquitin (Santa Cruz). We also transfected the indicated amounts of the plasmids encoding HA–ubiquitin (gift from S.H. Ryu, Postech, Korea) and p38 into 293 cells and incubated them for 16 h. We then extracted proteins from the transfected cells with RIPA buffer, immunoprecipitated FBP with antibody to FBP antibody and detected ubiquitinated FBP by western blotting with antibody to hemagglutinin (Santa Cruz). The deletion fragments of p38 were tested for their ability in degradation and ubiquitination of FBP as described in **Supplementary Methods** online.

Cell proliferation and differentiation. To determine the effect of p38 on cell proliferation, we transfected the indicated cell lines with the plasmid encoding p38, cultivated them for 48 h and then incubated them in fresh medium containing 1 μCi [³H]-thymidine for 4 h. After washing and lysing the cells with RIPA buffer, we quantified the amounts of the incorporated thymidine by liquid scintillation counting. To see the effect of p38 on lung cell differentiation, we isolated and chopped lungs from E17.5 embryos in PBS containing antibiotics and incubated them in 0.05% trypsin-EDTA for 2 h with agitation at 37 °C. After washing the isolated cells with ice-cold PBS, we cultivated them for 2 d in six-well plates. We mixed the p38 plasmid (2 μg) with 20 μl of adenovirus solution (A$_{280}$ = 0.05) and 50 μl of PBS and incubated it for 0.5 h at room temperature. We then added 50 μl of 40 μg ml^{-1} poly-L-lysine and 1 ml of DMEM containing 0.5% fetal bovine serum to the mixture and incubated for 1 h more at room temperature. We introduced this mixture to the PBS-washed primary lung cells. After 1 h incubation at 37 °C, we supplied the cells with 1 ml of 10% DMEM and incubated them for 36 h. Also, we cultivated A549 cells in RPMI 1640 medium, transfected them with 1 μg of p38 plasmid and incubated for 48 h. We extracted the cells with RIPA buffer, separated them by SDS–PAGE and immunoblotted them with the indicated antibodies.

Immunocytochemistry. To determine the cellular distribution of p38, we cultivated A549 cells to about 70% confluency on 5 × 5 mm coverslips and treated them with 2 ng ml^{-1} of TGF-β2 for 6 h. We then fixed the cells in 4%

paraformaldehyde for 30 min at 37 °C, washed them with PBS, incubated them in the PBS blocking solution containing 0.1% bovine serum albumin and 0.5% Triton X-100 at 4 °C for 1 h and reacted them with monoclonal antibody to p38 overnight at 4 °C. After washing the mixture, we incubated the cells with the antibody to mouse conjugated with fluorescein isothiocyanate for 90 min and stained the nuclear DNA with propidium iodide.

Note: Supplementary information is available on the Nature Genetics website.

1. Quevillon, S., Robinson, J.-C., Berthonneau, E., Siatecka, M. & Mirande, M. Macromolecular assemblage of aminoacyl-tRNA synthetases: identification of protein-protein interactions and characterization of a core protein. *J. Mol. Biol.* **285**, 183–195 (1999).
2. Kim, J.Y. *et al.* p38 is essential for the assembly and stability of macromolecular tRNA synthetase complex: implications for its physiological significance. *Proc. Natl. Acad. Sci. USA* **99**, 7912–7916 (2002).
3. Duncan, R. *et al.* A sequence-specific, single-strand binding protein activates the far upstream element of c-myc and defines a new DNA-binding motif. *Genes Dev.* **8**, 465–480 (1994).
4. Nicolaides, N.C., Kinzler, K.W. & Vogelstein, B. Analysis of the 5′ region of PMS2 reveals heterogeneous transcripts and a novel overlapping gene. *Genomics* **29**, 329–334 (1995).
5. Harding, H.P. *et al.* Regulated translation initiation controls stress-induced gene expression in mammalian cells. *Mol. Cell* **6**, 1099–1108 (2000).
6. Ben-Izhak, O. *et al.* Ki67 antigen and PCNA proliferation markers predict survival in anorectal malignant melanoma. *Histopathology* **41**, 519–525 (2002).
7. Semenza, G. Signal transduction to hypoxia-inducible factor 1. *Biochem. Pharmacol.* **64**, 993–998 (2002).
8. Griese, M. Pulmonary surfactant in health and human lung diseases: state of the art. *Eur. Respir. J.* **13**, 1455–1476 (1999).
9. Weaver, T.E. & Conkright, J.J. Function of surfactant proteins B and C. *Annu. Rev. Physiol.* **63**, 555–578 (2001).
10. Lawson, P.R. & Reid, K.B. The roles of surfactant proteins A and D in innate immunity. *Immunol. Rev.* **173**, 66–78 (2000).
11. Kalina, M., Mason, R.J. & Shannon, J.M. Surfactant protein C is expressed in alveolar type II cells but not in Clara cells of rat lung. *Am. J. Respir. Cell Mol. Biol.* **6**, 594–600 (1992).
12. Sugarara, K., Iyama, K., Sano, K. & Morioka, T. Differential expressions of surfactant protein SP-A, SP-B, and SP-C mRNAs in rats with streptozotocin-induced diabetes demonstrated by in situ hybridization. *Am. J. Respir. Cell Mol. Biol.* **11**, 397–404 (1994).
13. Wang, X., Avigan, M. & Norgren, R.B. Jr. FUSE-binding protein is developmentally regulated and is highly expressed in mouse and chicken embryonic brain. *Neurosci. Lett.* **252**, 191–194 (1998).
14. Duncan, R., Collins, I., Tomonaga, T., Zhang, T. & Levens, D. A unique transactivation sequence motif is found in the carboxyl-terminal domain of the single-strand-binding protein FBP. *Mol. Cell. Biol.* **16**, 2274–2282 (1996).
15. Davis-Smyth, T., Duncan, R.C., Zheng, T., Michelotti, G. & Levens, D. The far upstream element-binding proteins comprise an ancient family of single-strand DNA-binding transactivators. *J. Biol. Chem.* **271**, 31679–31687 (1996).
16. Zhou, M., Wu, X. & Ginsberg, H.N. Evidence that a rapidly turning over protein, normally degraded by proteasomes, regulates hsp72 gene transcription in HepG2 cells. *J. Biol. Chem.* **271**, 24769–24775 (1996).
17. Sanford, L.P. *et al.* TGFβ2 knockout mice have multiple developmental defects that are non-overlapping with other TGFβ knockout phenotypes. *Development* **124**, 2659–2670 (1997).
18. Kaartinen, V. *et al.* Abnormal lung development and cleft palate in mice lacking TGFβ3 indicates defects of epithelial-mesenchymal interaction. *Nat. Genet.* **11**, 415–421 (1995).
19. Markowitz, S. *et al.* Inactivation of the type II TGF-β receptor in colon cancer cells with microsatellite instability. *Science* **268**, 1336–1338 (1995).
20. Hannon, G.J. & Beach, D. p15INK4B is a potential effector of TGF-β-induced cell cycle arrest. *Nature* **371**, 257–261 (1994).
21. Hocevar, B.A., Brown, T.L. & Howe, P.H. TGF-β induces fibronectin synthesis through a c-Jun N-terminal kinase-dependent, Smad4-independent pathway. *EMBO J.* **18**, 1345–1356 (1999).
22. Liu, J. *et al.* The FBP interacting repressor targets TFIIH to inhibit activated transcription. *Mol. Cell* **5**, 331–341 (2000).
23. Guo, Q.M. *et al.* Identification of c-myc responsive genes using rat cDNA microarray. *Cancer Res.* **60**, 5922–5928 (2000).

24. Schuhmacher, M. *et al.* The transcriptional program of a human B cell line in response to Myc. *Nucleic Acids Res.* **29**, 397–406 (2001).

25. Ehrhardt, A. *et al.* Development of pulmonary bronchiolo-alveolar adenocarcinomas in transgenic mice overexpressing murine c-myc and epidermal growth factor in alveolar type II pneumocytes. *Br. J. Cancer* **84**, 813–818 (2001).

26. Chinoy, M.R., Chi, X. & Cilley, R.E. Down-regulation of regulatory proteins for differentiation and proliferation in murine fetal hypoplastic lungs. *Pediatr. Pulmonol.* **32**, 129–141 (2001).

27. Todaro, G.J. & Green, H. Quantitative studies of the growth of mouse embryo cells in culture and their development into established lines. *J. Cell Biol.* **17**, 299–313 (1963).

28. Kang, J. *et al.* Heat shock protein 90 mediates protein-protein interactions between human aminoacyl-tRNA synthetases. *J. Biol. Chem.* **275**, 31682–31688 (2000).

29. Rho, S.B. *et al.* Genetic dissection of protein-protein interactions in multi-tRNA synthetase complex. *Proc. Natl. Acad. Sci. USA* **96**, 4488–4493 (1999).